2011

A systematic study of neutral and charged 3d-metal trioxides and tetraoxides

Kalpataru Pradhan
Virginia Commonwealth University

Gennady L. Gutsev
Florida Agricultural and Mechanical University

Charles A. Weatherford
Florida Agricultural and Mechanical University

Puru Jena
Virginia Commonwealth University, pjena@vcu.edu

Pradhan, K., Gutsev, G.L., Weatherford, C.A., et al. A systematic study of neutral and charged 3d-metal trioxides and tetraoxides. The Journal of Chemical Physics, 134, 144305 (2011).

A systematic study of neutral and charged 3d-metal trioxides and tetraoxides

Kalpataru Pradhan,[1] Gennady L. Gutsev,[2] Charles A. Weatherford,[2] and Purusottam Jena[1,a)]

[1]*Department of Physics, Virginia Commonwealth University, 701 West Grace Street, Richmond, Virginia 23284-2000, USA*

[2]*Department of Physics, Florida A&M University, Tallahassee, Florida 32307, USA*

(Received 29 November 2010; accepted 4 March 2011; published online 11 April 2011)

Using density functional theory with generalized gradient approximation, we have performed a systematic study of the structure and properties of neutral and charged trioxides (MO_3) and tetraoxides (MO_4) of the 3d-metal atoms. The results of our calculations revealed a number of interesting features when moving along the 3d-metal series. (1) Geometrical configurations of the lowest total energy states of neutral and charged trioxides and tetraoxides are composed of oxo and/or peroxo groups, except for CuO_3^- and ZnO_3^- which possess a superoxo group, CuO_4^+ and ZnO_4^+ which possess two superoxo groups, and CuO_3^+, ZnO_3^+, and ZnO_4^- which possess an ozonide group. While peroxo groups are found in the early and late transition metals, all oxygen atoms bind chemically to the metal atom in the middle of the series. (2) Attachment or detachment of an electron to/from an oxide often leads to a change in the geometry. In some cases, two dissociatively attached oxygen atoms combine and form a peroxo group or a peroxo group transforms into a superoxo group and vice versa. (3) The adiabatic electron affinity of as many as two trioxides (VO_3 and CoO_3) and four tetraoxides (TiO_4, CrO_4, MnO_4, and FeO_4) are larger than the electron affinity of halogen atoms. All these oxides are hence superhalogens although only VO_3 and MnO_4 satisfy the general superhalogen formula. © *2011 American Institute of Physics*. [doi:10.1063/1.3570578]

I. INTRODUCTION

Different oxidation states of 3d-metals give rise to a variety of metal clusters containing oxygen.[1–3] Transition metal oxides are widely used as catalysts[4] and are of the paramount importance in organometallic, biocatalysis, and surface sciences. From a practical point of view, it is important to identify the reactive sites in heterogeneous catalysis,[5] which stimulated the studies of neutral and anionic clusters in the gas phase.[6] In addition, transition metal oxide ions play an important role in atmospheric chemistry where they act as nucleation centers and oxidizing agents.[7,8]

A systematic study of MO and MO_2 (M = 3d-metal atoms) and their negative ions has been carried out previously.[9,10] The electron affinities of the monoxides are relatively small and do not exceed 2 eV. The ground-state geometries of MO_2 are found to possess the oxo form except for CuO_2 and ZnO_2. Copper dioxide has the lowest total energy state with a superoxo geometrical configuration; whereas O_2 dissociates from Zn atom during geometry optimizations of ZnO_2. The ground-state electronic configuration of Cu is $3d^{10}4s^1$ and, correspondingly, the Cu atom has a single valence electron. Consequently, a Cu atom interacts with only one oxygen atom and forms a superoxo configuration. A Zn atom has a $3d^{10}4s^2$ electronic configuration and does not form thermodynamically stable states when interacting with O_2. The geometry of ZnO_2 reported[10] is linear OZnO and the corresponding state is metastable. The ground-state geometry of both CuO_2^- and ZnO_2^- has the oxo form similar to that in the rest of the MO_2^- anions. The electron affinities of the 3d-metal dioxides are larger than those of the monoxides and exceed 3 eV for the late transition metal dioxides.

The shape of the MO_2 ground-state geometries shows that all 3d-metal atoms from Sc to Ni are capable of cleaving O_2. The ground-state NiO_2 neutral is thermodynamically less stable than all other neutral dioxides with the oxo geometries. This is reflected in the high electron affinity of NiO_2, which exceeds 3 eV. The formal valence of Ti is 4 and matches the sum of valencies of two oxygen atoms. This can explain why TiO_2 is the most thermodynamically stable dioxide in the 3d-metal dioxide series. Correspondingly, the TiO_2 electron affinity is smaller than the electron affinity of all other metal dioxides. The adiabatic electron affinities of NiO_2, CuO_2, and ZnO_2 are larger than 3 eV being somewhat smaller than the electron affinity of the Cl atom (3.62 eV).

It has previously been demonstrated that molecules composed of a metal atom (M) surrounded by electronegative ligand atoms (X) can possess electron affinities which are higher than the electron affinity of halogen atoms.[11,12] Such species were named "superhalogens." A superhalogen has a general formula $MX_{(n+1)/m}$, where n is the maximal formal valence of the central atom and m is the normal valence of the electronegative atom X.[13,14] LiX_2,[15] MgX_3,[16] and ScX_4 (Refs. 17 and 18) (X = Cl, F) satisfy the above formula and present examples of superhalogens.

Our previous density functional calculations were performed for the neutral and negatively charged CrO_n,[19] MnO_n,[20,21] and FeO_n (Ref. 22) for n = 3 and 4. All three

a)Electronic mail: pjena@vcu.edu.

MO_4 neutrals were found to be superhalogens, whereas only MnO_4 satisfies the above superhalogen formula and possesses the largest electron affinity in the MO_4 series. Among the 3d-metal trioxides, only VO_3 satisfies the superhalogen formula and it was experimentally confirmed to be a superhalogen.[23] However, many other oxides may possess electron affinities, which exceed the electron affinity of F or Cl atoms. In our recent study,[24] we found FeO_{12} cluster to be geometrically stable with the adiabatic electron affinity of 3.69 eV, which is close to the adiabatic electron affinity of FeO_4. It is interesting to find out how the electron affinity depends on the number of oxygen atoms and the central atom in other 3d-metal oxides.

This work presents a systematic study of the structure, electron affinities, ionization energies, and thermodynamic stability of the MO_n clusters (M = Sc to Zn; n = 3, 4) aimed at establishing the trends in the structures and properties when moving along the MO_3 and MO_4 series. In the 3d-metal atoms, the magnetic moment increases from Sc to Mn and then drops to 0 at Zn; therefore, it is interesting to reveal the ability of oxygen to quench these moments when three or four oxygen atoms are added. Another interesting question is how the attachment or detachment of an electron influences the geometry and the total magnetic moment in the MO_3 and MO_4 series. In Sec. II, we outline our theoretical procedure; Sec. III describes the changes in the structures and binding energies when moving along the neutral and singly charged MO_3 series. We discuss the properties of the neutral and charged tetraoxides in Sec. IV, and compare our results obtained for the MO_3 and MO_4 series in Sec. V.

II. COMPUTATIONAL DETAILS

Our calculations are performed using density functional theory with generalized gradient approximation (DFT-GGA). The exchange-correlation functional is composed from the Becke's exchange[25] and Perdew–Wangs correlation[26], known as the BPW91 functional. The choice of this functional, among many others available nowadays,[27–29] is based on our previous assessments of this functional for 3d-metal oxides,[10,24] and the BPW91 stability in harmonic frequency calculations of closely spaced states of iron clusters.[30] The BPW91 functional is found to produce the results which are quite close to those obtained using the coupled-cluster method with singles and doubles and noniterative inclusion of triples [CCSD(T)] (Ref. 31) for $(TiO_2)_n$ clusters,[32] $(CrO_3)_n$ clusters,[33,34] and FeO_2.[35] Good agreement between the BPW91 and experimental data was obtained for $Cr_3O_8^-$.[36]

The atomic orbitals are represented by the Gaussian basis sets 6–311+G(3df) [metal atoms: (15s11p6d3f1g/10s7p4d3f1g) and O: (12s6p3d1f/5s4p3d1f)].[37,38] The geometries were first optimized without any symmetry constraint using the GAUSSIAN 03 code.[39] Different trial geometries, where oxygen atoms are bound to the metal atom molecularly (peroxo or superoxo), dissociatively (oxo), and as an ozonide, were probed in order to arrive at the ground-state geometries. All possible spin multiplicities were tried in order to determine the total spin of the ground state. The lowest energy states found were reoptimized with symmetry constraints corresponding to the actual nuclear symmetry derived from the results of our symmetry unconstrained optimizations. The convergence threshold for total energy was set to 0.000001 eV and the force threshold was set to 0.001 eV/Å. Harmonic vibrational frequencies of all states are positive, which means that these states correspond to the potential energy surface minima.

The adiabatic electron affinity (EA_{ad}) is calculated as the difference between total energies, comprised of the total electronic energy and zero point vibrational energy (ZPVE), of a neutral and the corresponding anion at their respective ground-state geometries. Similarly, the adiabatic ionization energy (IE) is computed as the difference between total energies of a cation and the corresponding neutral at their respective ground-state geometries. The vertical detachment energy (VDE) of an extra electron from an anion is computed as the difference in total electronic energies between an anion and its neutral parent at the anion geometry. Similarly, the vertical ionization energy (VIE) is computed as the difference in total electronic energies between a cation and its neutral parent computed at the neutral geometry.

III. TRIOXIDES

A. Neutral MO_3

The ground-state geometries of MO_3 displayed in Fig. 1 do change when moving from ScO_3 to ZnO_3. In order to understand these changes, we resort to the ground-state geometries of neutral MO_2.[10] All dioxide geometries have an oxo form except for CuO_2, which has a superoxo form. Formally, each oxygen atom is divalent since it requires two electrons to fill up its 2p shell. The Sc atom has three valence electrons; nonetheless, its interaction with two oxygen atoms leads to an oxo geometrical configuration of the lowest energy state in ScO_2. The Cu atom in CuO_2 has the electronic configuration close to $3d^{10}4s^1$ with a single valence electron; therefore, it is natural for oxygen in CuO_2 to form a peroxo group. Formally, a Zn atom with a $3d^{10}4s^2$ electronic configuration can be considered as divalent. However, the Zn atom prefers to conserve its closed shell and not to attach to O_2 either in peroxo or superoxo form.

In the trioxide series, the formal valence of Sc (3) and Ti (4) is insufficient for the dissociative attachment of three oxygen atoms. Consequently, there are peroxo and oxo groups in the lowest total energy states of ScO_3 and TiO_3. Beginning with V, all MO_3 up to M = Co have a trioxo form. Due to a decrease in the valence at the end of the 3d-metal series, the geometries of NiO_3, CuO_3, and ZnO_3 are similar to the ScO_3 geometry and possess one peroxo and one oxo group.

The existence of thermodynamically stable CuO_3 and ZnO_3 is very surprising since CuOO is barely stable while ZnOO is dissociative. Apparently, the addition of an oxygen atom to CuOO or metastable OZnO increases the formal valence of the central atom. This behavior can be related to the strong ionic character of bonding in the 3d-metal trioxides, as follows from the results of the natural bond orbital (NBO) analysis,[40] which uses the basis of natural atomic orbitals. The effective electronic configuration of Cu in the quartet ground state of CuO_3 is $3d^{9.52}4s^{0.49}$, which corresponds to a

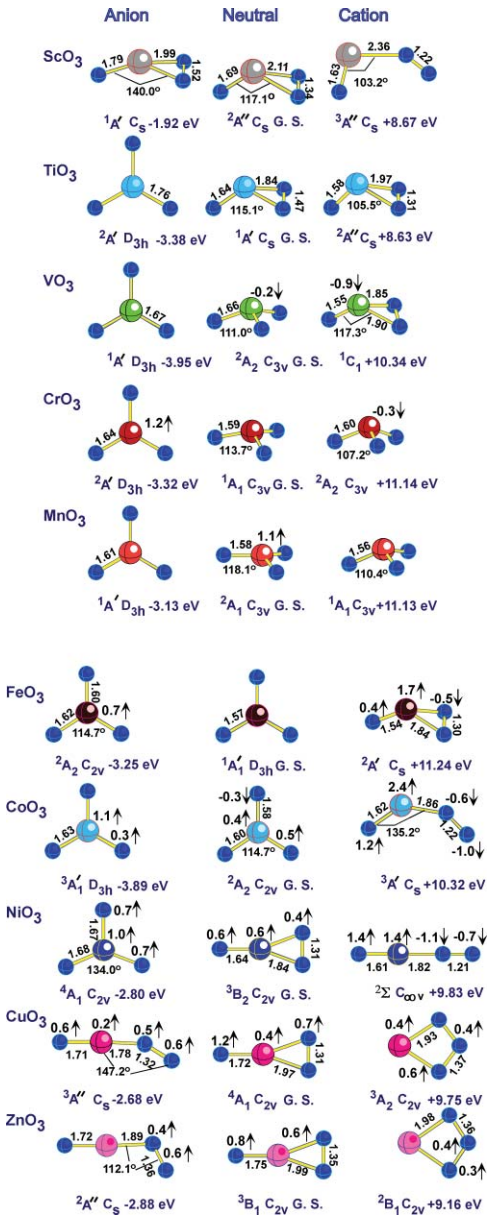

FIG. 1. Optimized geometrical configurations of the anionic, neutral, and cationic MO_3 ground states. Bond lengths are in angstroms (Å), excess spin density on atoms are in electrons.

promotion of 1/2 of an electron into the oxo and peroxo group each. The effective electronic configuration of Zn in the triplet ground state of ZnO_3 is $3d^{9.91}4s^{0.62}$. One electron is promoted to the oxo oxygen and about 1/2 of an electron is promoted to the superoxo group.

The magnetic moment of the central atom is quenched in the ground-state trioxides up to CoO_3. The total magnetic moment of trioxides from ScO_3 to CoO_3 is either 0 or 1 μ_B, depending on the parity of the 4s + 3d electron number (see Table I), which corresponds to the spin multiplicities of 1 or 2, respectively. This may be related to the number of valence electrons in Sc, Ti, V, and Cr which is less than or equal to the sum of three oxygen valencies. The number of Mn valence electrons is 7 and the total magnetic moment of MnO_3 is 1 μ_B. Ground-state iron and cobalt atoms have the formal

TABLE I. The EA_{ad}, VDE, IE, VIE values and the total magnetic moments, M, of the neutral, anionic, and cationic trioxides.[a]

	Neutral	Anion	Cation					
Cluster	M	M	M	EA_{ad}	VDE	Exp.[b]	IE	VIE
ScO_3	1	0	2	1.92	2.61		8.67	9.43
TiO_3	0	1	1	3.38	4.24	4.2 ± 0.1	8.63	9.39
VO_3	1	0	0	3.95	4.16	4.36 ± 0.05	10.34	11.40
CrO_3	0	1	1	3.32	3.53	3.66 ± 0.02	11.14	11.34
MnO_3	1	0	0	3.13	3.18	3.21 ± 0.01	11.13	11.41
FeO_3	0	1	1	3.25	3.37	3.26 ± 0.04	11.24	11.42
CoO_3	1	2	2	3.89	4.04		10.32	11.61
NiO_3	2	3	1	2.80	3.66		9.83	10.08
CuO_3	3	2	2	2.68	3.06	3.19 ± 0.04	9.75	10.31
ZnO_3	2	1	1	2.88	3.11		9.16	9.96

[a]All values are in eV except for the total magnetic moment values, which are in Bohr magnetons μ_B.
[b]See the experimental references in the text.

valence of 8 and 9 with the magnetic moments of 4 μ_B and 3 μ_B, respectively. These magnetic moments are quenched in the corresponding trioxides. Surprisingly, the total magnetic moments of trioxides CuO_3 (3 μ_B) and ZnO_3 (2 μ_B) are larger than the magnetic moments of Cu (1μ_B) and Zn (0μ_B) atoms, respectively, i.e., the oxidation increases the total magnetic moment of these trioxides. The excess spin densities, which correspond to the local magnetic moments, at the metal site exceed 0.2e in MnO_3 (1.1e), CoO_3 (0.4e), NiO_3 (0.6e), CuO_3 (0.4e), and ZnO_3 (0.4e) [see Fig. 1].

Our results obtained for the neutral MO_3 species are in good agreement with the results of previous theoretical work performed in order to assign experimental IR frequencies of species trapped in inert matrices.[2] The previous work used mainly the hybrid Hartree–Fock-density-functional-theory (HFDFT) approach B3LYP and smaller basis sets than the basis set we used in the present work. The ground-state structures of ScO_3,[41] TiO_3,[42,43] CrO_3,[44,45] MnO_3,[46] FeO_3,[47] NiO_3,[48] and CuO_3 (Ref. 49 and 50) along with their computed total magnetic moments are similar to those obtained from our calculations. Our results are; however, different for VO_3 and CoO_3. The former neutral was previously found to have a trigonal planar geometry of C_{2v} symmetry[51] while we obtained a slightly distorted D_{3h} nonplanar geometry of C_{3v} geometry, in agreement with the results of previous DFT-GGA (Ref. 52) and quantum Monte-Carlo[53] calculations. CoO_3 was previously found to possess the $^6A_1$ oxo-peroxo ground state at the HFDFT B1LYP/6–311+G* level,[54] whereas our calculations predict all oxygen to be bound dissociatively in the $^2A_2$ ground state (see Fig. 1). No data were reported for ZnO_3 to the best of our knowledge.

Thermodynamic stability of the neutral MO_3 clusters is estimated by comparing the O and O_2 loss energies, which are computed according to

$$\Delta E_{tot} = E_{tot}(MO_n) - E_{tot}(MO_{n-m}) - E_{tot}(O_m),$$
$$n = 3,\ 4;\ m = 1,\ 2, \quad (1)$$

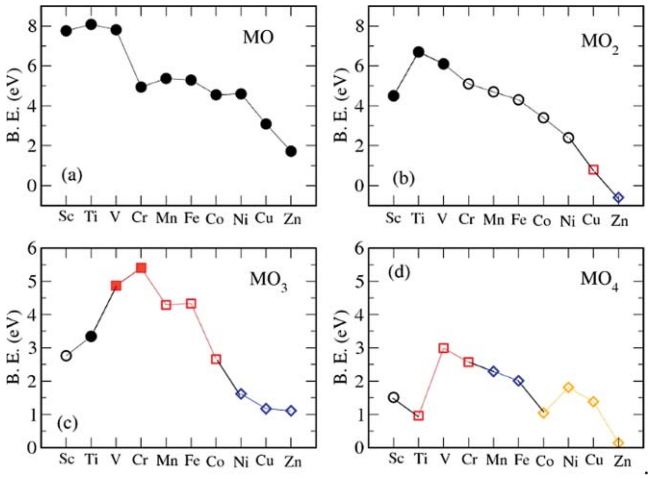

FIG. 2. Fragmentation energies (in eV) of the MO, MO_2, MO_3, and MO_4 series. The filled symbols indicate the atomic oxygen release and open symbols are for the molecular oxygen release. Different colors serve as the indicators of changes in the geometrical shape when moving along the series.

where E_{tot} includes the ZPVE correction. The smallest dissociation energies in the MO_3 and MO_4 series computed according to Eq. (1) are plotted in Fig. 2 together with the dissociation energies of the monoxides and dioxides from our previous work.[9,10] In the monoxide series, ScO, TiO, and VO are significantly more stable compared to the rest of the series, which is related to the formation of triple bonds through a dative mechanism in these monoxides.[55] The smallest energy decay channel in the MO_3 series corresponds to the molecular oxygen release, except for TiO_3, VO_3, and CrO_3 where the yield of atomic oxygen is preferred.

In the MO_2 series, the most thermodynamically stable species is TiO_2 that correlates with 4 valence electrons of Ti. In the MO_3 series, CrO_3 is the most stable species that correlates with the maximum formal valence of 6 of the Cr atom. By analogy, FeO_4 should be the most stable member of the MO_4 series. However, it is not so and the most thermodynamically stable is VO_4. This "anomaly" can be related with the geometrical shape of VO_4, which is found to be of the dioxo-peroxo type. If one accepts the formal valence of a peroxo group to be 1, then the sum of oxygen valencies matches the formal valency of V atom.

B. MO_3^- anions

In the MO_3 series, VO_3 should possess the largest adiabatic electron affinity according to the superhalogen formula, and indeed its computed EA_{ad} of 3.95 eV is the largest EA_{ad} in the 3d-metal trioxide series. The computed vertical ionization energy of 4.16 eV of the VO_3^- anion is in good agreement with the experimental value of 4.36 ± 0.05 eV.[23] The ground state of the VO_3^- anion is a singlet with an equilateral triangle geometrical configuration of D_{3h} symmetry (see Fig. 1). As it is seen from Fig. 1, the attachment of an extra electron changes the geometrical shape of the trioxide anions of Ti, Cu, Ni, and Zn. In these species, the extra electron breaks either the bond between two oxygen atoms or the bond between the metal atom and an oxygen atom. Similar to the geometries

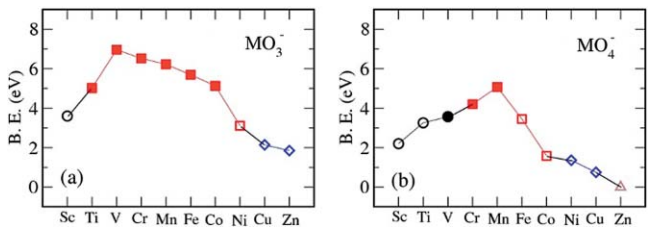

FIG. 3. Fragmentation energies (in eV) of the MO_3^- and MO_4^- anions corresponding to the atomic (solid symbols) or molecular oxygen release. Different colors in (a) indicate different geometries shown in Fig. 1.

of the neutral parents, the anionic geometries are changing in the beginning and in the end of the series when moving from ScO_3^- to ZnO_3^-. The anion tri-oxo group is preferred from TiO_3^- to NiO_3^-.

Estimations of the anion thermodynamic stability require energy evaluations for four dissociation channels:

$$\Delta E_{tot,anion} = E_{tot}(MO_n^-) - E_{tot}(MO_{n-m}^-) - E_{tot}(O_m), \quad n = 3,\ 4;\ m = 1,\ 2, \tag{2}$$

$$\Delta E_{tot,anion} = E_{tot}(MO_n^-) - E_{tot}(MO_{n-m}) - E_{tot}(O_m^-), \quad n = 3,\ 4;\ m = 1,\ 2. \tag{3}$$

The smallest dissociation energies obtained from Eqs. (2) and (3) are displayed in Fig. 3(a). These energies correspond to the release of atomic or molecular oxygen except for TiO_3^-, where the smallest energy channel corresponds to the release of an O^- ion. This peculiarity can be related to the high thermodynamic stability of neutral TiO_2. The superhalogen anion VO_3^- is the most thermodynamically stable species among the 3d-metal trioxide anions. All the anions marked in the figure by square symbols have the oxo form and are expected to eject atomic oxygen rather than molecular oxygen except for NiO_3^-, for which the molecular oxygen yield is preferred.

The calculated vertical detachment energies (VDEs) of an extra electron from the MO_3^- anions and the EA_{ad}s of the neutral 3d-metal trioxides are compared with experiment in Table I and visualized in Fig. 4(a). The VDE and EA_{ad} values are rather close to each other for VO_3, CrO_3, MnO_3, FeO_3, and CoO_3. This is consistent with small geometry changes due to an extra electron attachment (see Fig. 1). The VDE and EA_{ad} values of TiO_3 and NiO_3 are quite different, which can be related to the different shape of the corresponding neutral and anionic geometries. Both ScO_3 and ScO_3^- possess the same geometrical topology; however, there is a significant difference between the VDE and EA_{ad} values. The noticeable elongation of interatomic distances in the ScO_3^- anion can explain this difference. On the contrary, the differences between the VDE and EA_{ad} values of in case of Cu and Zn trioxides are quite small despite they have the geometrical topologies, which are different from those in the corresponding anions.

As it is seen from Table I, the EA_{ad}s of VO_3 and CoO_3 are larger than the EA of the Cl atom. VO_3, with a $3d^3 4s^2$ valence

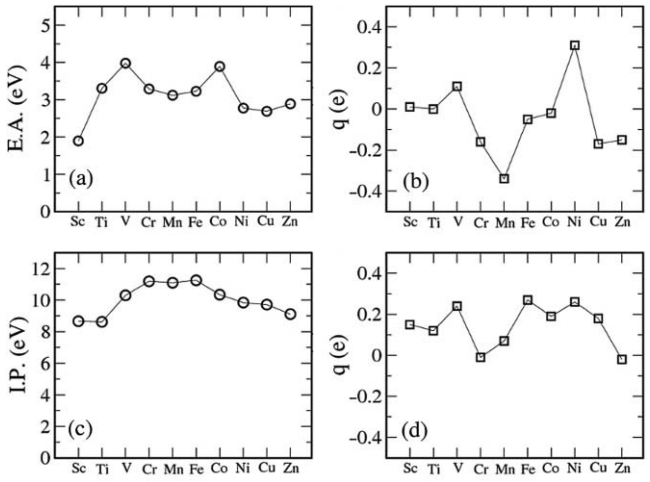

FIG. 4. The MO_3 series: (a) adiabatic electron affinities; (b) differences in the charges of the metal atoms in the MO_3^- – MO_3 pairs; (c) ionization energies; (d) the metal atom charge differences in the MO_3 – MO_3^+ pairs.

electronic configuration of the ground-state metal atom, satisfies the superhalogen formula, while Co possesses a $3d^74s^2$ electronic configuration and its superhalogen has to be CoO_5. According to the NBO analysis, Co possesses the effective electronic configurations of $3d^{7.48}4s^{0.36}$ and $3d^{7.49}4s^{0.37}$ in CoO_3 and CoO_3^-, respectively. This means that the extra electron is entirely delocalized over the oxygen atoms, similar to that in VO_3^-. Therefore, the CoO_3 EA_{ad} increase with respect to the EA_{ad}s of the neighbor trioxides may be related to a stronger Coulomb attraction exerted by the central atom in the CoO_3^- anion. An extra electron attachment to TiO_3 breaks the peroxo bond and the negative ion has D_{3h} symmetry. This can explain why the EA_{ad} of TiO_3 exceeds the EA_{ad} of ScO_3 by 1.41 eV. Experimental data for TiO_3,[56] VO_3,[23] CrO_3,[19] MnO_3,[20] FeO_3,[57] and CuO_3 (Ref. 49) are also given in Table I.

The charges on metal atoms are always positive according to our NBO analysis, which is due to the charge transfer from the central atom to oxygen atoms in all MO_3 clusters. The charges on the metal atoms in the MO_3^- anions are given in Fig. 4(b) relative to the charges on the metal atoms in the neutral MO_3 series. As it is seen, there is no significant difference in the metal atom charge in most cases. The metal atom charge in MnO_3^- and NiO_3^- has the largest deviation which; however, does not exceed 0.4 e.

The total ground-state magnetic moments of the MO_3^- anions are quenched to either 0 or 1 μ_B depending on the electron number parity except for the trioxide anions of Co, Ni, and Cu. The total magnetic moment of CoO_3^- and NiO_3^- increases by one as compared to the total magnetic moments of the corresponding neutral parents and decreases by one in the CuO_3^- anion. Our anion ground-state assignment is similar to that obtained in the previous CCSD(T) computations[58] of TiO_3^-, complete active space with second-order perturbation theory computations[59] of FeO_3^-, and previous DFT-GGA computations of CuO_3^-,[60,61] but is different from the B3LYP assignment[62] of a $^2B_2$ (C_{2v}) ground state for TiO_3^-.

C. MO_3^+ cations

The electronic structure of the 3d-metal mono and dioxide cations was the subject of a number of experimental and theoretical studies.[63–66] This section extends these studies to the 3d-metal trioxide cations. The ground states of MO_3^+ are presented in Fig. 1 along with those of the corresponding neutrals and anions. As it is seen, the electron detachment results into a conversion of the peroxo groups of ScO_3 and NiO_3 as well as two oxo atoms of CoO_3 into the corresponding superoxo groups, whereas two oxo atoms of VO_3 and FeO_3 transform into the peroxo groups. The most dramatic changes are found for CuO_3^+ and ZnO_3^+, where the peroxo and oxo groups recombine into the ozonide group. Thus, the electron detachment from a neutral trioxide either breaks the bond between metal and oxygen atoms or brings two oxygen atoms closer. Similar to the neutral and anionic series, the cation geometries do change when moving from ScO_3^+ to ZnO_3^+. It is worth to note that the bond length between oxygen atoms in the peroxo group of ScO_3^+, CoO_3^+, and NiO_3^- matches the bond length of 1.22 Å in the gas phase dioxygen.

The calculated adiabatic (IE) and vertical (VIE) ionization energies of the neutral trioxides are presented in Table I. The IE and VIE values of CrO_3 and MnO_3 are close to each other, which is consistent with the small geometry changes due to the electron detachment [see Figs. 1 and 4(c)]. The differences between the IE and VIE values of other trioxides are considerably larger because of significant differences between the neutral and cationic geometries, except for FeO_3 and NiO_3, whose IE and VIE values are close to each other despite significant structural differences between the corresponding neutral and cationic geometrical configurations.

The charges on metal atoms in the MO_3^+ cations obtained from the NBO analysis are given in Fig. 4(d) relative to the charges on the metal atom in the MO_3 neutrals. As it is seen, there is no significant difference in the charges when moving along the cation series. The largest deviation does not exceed 0.3e, which implies that the detached electron originates from the oxygen atoms. The total magnetic moments of the ground-state MO_3^+ cations are either 0 or 1 μ_B, except for ScO_3^+, CoO_3^+, and CuO_3^+, which have the triplet ground states. The local magnetic moments at the metal sites of FeO_3^+ (1.7 μ_B), CoO_3^+ (2.4 μ_B), and NiO_3^+ (1.4 μ_B) are the largest local magnetic moments among all the neutral and charged trioxides.

Experimental vibrational frequencies were obtained[67,68] for VO_3^+, whose structure was optimized in the accompanying B3LYP/TZVP calculations. The assigned ground state $^3A''$ (C_s) is different from the previous assignment of $^1A'$ (C_s) obtained from the B3LYP/31G* and B3LYP/TZV optimizations.[69,70] The experimental vibrational frequencies of 1037 and 1069 cm^{-1} are in rather poor agreement with the B3LYP frequencies of the both states (1161 and 1228 cm^{-1} in the $^3A''$ state; 1040 and 1178 cm^{-1} in the $^1A'$ state). The VO_3^+ ground-state assignment is quite complicated because there are at least three closely spaced states: a singlet state without symmetry shown in Fig. 1, where the excess spin density of 0.9 μ_B at V is antiferromagnetically coupled to the excess spin densities of the oxygens; a nonmagnetic $^1A'$ (C_s)

state whose total energy is practically the same as the previous state total energy; and a nonmagnetic $^3A''$ (C_s) state which is above the $^1A'$ state by 0.03 eV at the BPW91/6–311+G(3df) level. Harmonic vibrational frequencies of 1084 and 1112 cm^{-1} obtained for the nonsymmetric singlet state of VO_3^+ are in relatively good agreement with the experiment (note that the spectra were obtained in He_2 matrices); however, the intensity ratio of 1:4.6 is far off the experimental ratio of 1:1.6.

IV. TETRAOXIDES

A. Neutral MO_4

The optimized ground-state geometries of the neutral 3d-metal tetraoxides are displayed in Fig. 5. The ground-state geometry of the first member of the series, ScO_4, contains two peroxo groups. A peroxo group transforms into two oxo atoms in TiO_4, VO_4, and CrO_4, and the second peroxo group transforms into two oxo atoms in MnO_4. The structures of FeO_4 and MnO_4 are similar and correspond to all four oxygen atoms bound dissociatively; however, these states are nearly degenerate in total energy with the states possessing dioxo-peroxo geometries. Beginning with CoO_4, all tetraoxides have diperoxo geometrical ground-state configurations, where one peroxo-group rotates with respect to another one that results in D_2, D_{2h}, or D_{2d} symmetry. A geometrically stable isomer of ZnO_4 shown in Fig. 5 is thermodynamically metastable because the sum of total energies of Zn and two separated oxygen molecules is lower by ~0.1 eV than the ZnO_4 total energy. The total magnetic moments of the neutral tetraoxides MO_4 where M = Sc, V, Cr, Mn, Fe, and Cu are either 0 or 1 μ_B. The largest magnetic moment of 3 μ_B is found for CoO_4, and the ground states of the neutral Ti, Ni, and Zn tetraoxides are triplets. Local magnetic moments of the 3d-metal atoms in the neutral tetraoxides do not exceed 0.3 μ_B except for Ni, whose magnetic moment is 1.5 μ_B.

Figure 2(d) presents the smallest fragmentation energies of the neutral tetraoxides computed according to Eq. (1). The number of valence electrons of Fe is 8 and matches the sum of formal valencies of dissociatively bound oxygen atoms. One could anticipate that FeO_4 is the most thermodynamically stable cluster in the neutral tetraoxide series, but it is not so. We found VO_4 with five valence electrons of V to be the most thermodynamically stable cluster in the series. FeO_4 is also less thermodynamically stable than MnO_4, which is consistent with an assignment of a smaller oxidation number[71] to Fe than to Mn (6 and 7, respectively). A sudden decrease in the fragmentation energy of TiO_4 as compared to the fragmentation energies of its neighbors ScO_4 or VO_4 can be attributed to the high thermodynamic stability of the TiO_2 dioxide.

The CrO_4,[19] NiO_4,[48] and CuO_4 (Ref. 72) ground-state geometrical structures identified on the basis of laser photodetachment data match the corresponding structures obtained in the present work. The lowest total energy $^2A_2$ state of ScO_4 found previously at the B3LYP level has the geometry of C_{2v} symmetry[73] where one peroxo group is perpendicular to the second peroxo group. According to our optimizations, the $^2A''$ ground-state geometry of ScO_4 also has two peroxo groups but the geometrical configuration has C_s symmetry with slightly different bond lengths in the peroxo groups (see Fig. 5). The $^2A_2$ (C_{2v}) state is above this $^2A''$ state by only 0.03 eV in total electronic energy and has an imaginary frequency of −108i.

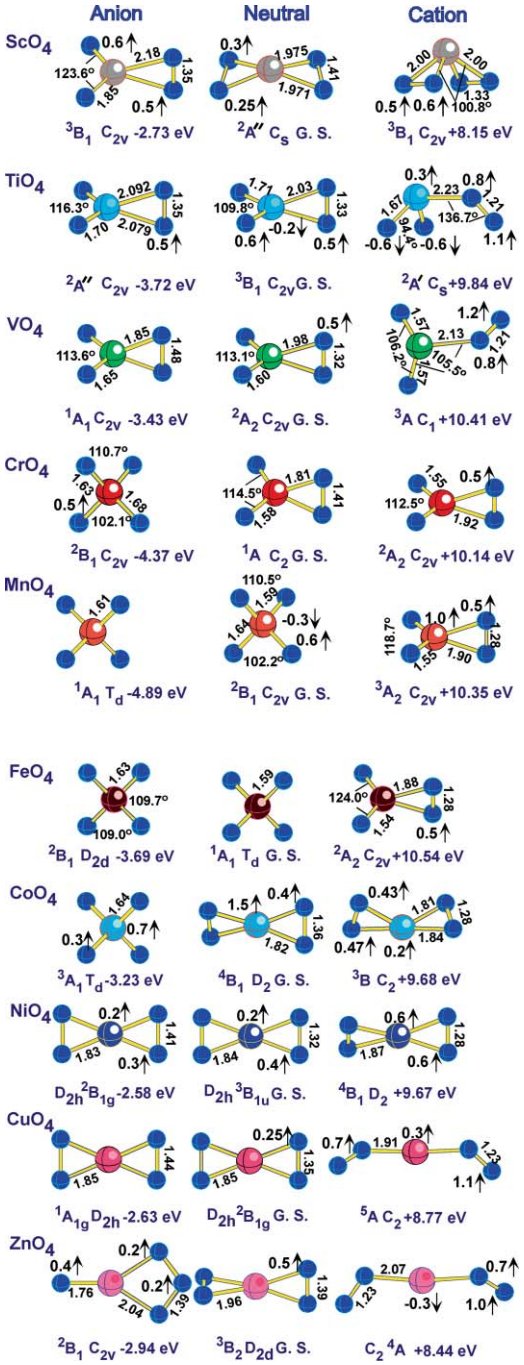

FIG. 5. Optimized geometrical configurations of the anionic, neutral, and cationic MO_4 ground states. Bond lengths are in angstroms (Å), excess spin density on atoms are in electrons.

Our ground-state structure of VO_4 found in our calculations is the same as reported previously.[74,75] According to the results of B3LYP calculations,[76] MnO_4 has a dioxo-peroxo geometrical structure similar to that of VO_4, whereas we found MnO_4 to possess a tetragonal geometry of C_{2v} symmetry, which is in accord with the photoelectron spectroscopic

(PES) study.[21] According to the tentative PES assignment,[77] FeO_4 has a dioxo-peroxo geometrical structure similar to that of VO_4 while we found that the lowest total energy states of both FeO_4 and FeO_4^- possess tetragonal geometrical configurations. The contradiction was attributed[78] to the presence of two isomers in the experimental anion flow, which produce two major peaks at ~3.2 and ~3.7 eV. CoO_4 was previously found to have a dioxo-peroxo geometrical configuration of C_{2v} symmetry,[79] while our calculations predict a diperoxo configuration of D_2 symmetry. This is very surprising, since both calculations are performed at the same BPW91/6–311+G(3df) level. Our optimizations show the $^2A_2$ state to be above the $^4B_1$ (D_2) state displayed in Fig. 5 by 0.2 eV. In agreement with the previous studies,[50,80] CuO_4 has a diperoxo ground-state structure of D_{2h} symmetry. No data are found for ZnO_4.

B. MO_4^- anions

The ground states of 3d-metal tetraoxide anions are presented in Fig. 5. With respect to the neutral parent geometries, the peroxo groups of ScO_4^- and CrO_4^- are split into two oxo groups and both peroxo groups of CoO_4^- are split into four oxo atoms. The ZnO_4^- anion is geometrically stable at the diperoxo geometry shown in Fig. 5; however, this anion is unstable thermodynamically since its total energy is higher by 0.18 eV than the sum of total energies of ZnO_2^- and O_2. Similar to the neutral tetraoxides, the anion geometries do change when moving from ScO_4^- to ZnO_4^-. The ScO_4^-, TiO_4^-, and VO_4^- anions possess one peroxo group, whereas all oxygen atoms are attached dissociatively in CrO_4^-, MnO_4^-, FeO_4^-, and CoO_4^-. The NiO_4^- and CuO_4^- ground-state geometries are similar and have a diperoxo shape.

The smallest fragmentation energies of MO_4^- computed according to Eqs. (2) and (3) are displayed in Fig. 3(b). As expected, MnO_4^- is the most thermodynamically stable anion in the series. We found the atomic oxygen yield to be preferred in VO_4^-, CrO_4^-, and MnO_4^-. For ScO_4^-, TiO_4^-, and the anions in the end of the series, the smallest energy fragmentation channel corresponds to the dioxygen release.

The calculated VDEs of the MO_4^- anions and the EA_{ad}s of their neutral parents are collected in Table II. The EA_{ad} and VDE values are quite close to each other for tetraoxides of Ti, Mn, Fe, Ni, and Cu, which is consistent with the small geometry changes resulting from an extra electron attachment (see Fig. 5). The geometries of neutral ScO_4, CrO_4, and CoO_4 are different from those of the corresponding anions. Consequently, the differences between the corresponding VDE and EA_{ad} values are larger. An indirect confirmation of a large change in the geometries of the ScO_4 and ScO_4^- pair follows from the laser photodetachment spectra[81] of ScO_4^-, where a wide featureless peak was observed in the area above 3 eV. The VO_4 and VO_4^- pair presents an exception since the difference between the EA_{ad} and VDE is quite large whereas both species have the same topology. However, one can notice rather drastic changes in the bonds of the peroxo group; namely, R(V – O) and R(O – O) are larger in the anion than in the neutral parent by 0.13 and 0.16 Å, respectively. The

TABLE II. The EA_{ad}, VDE, IE, VIE values and the total magnetic moments, M, of the neutral, anionic, and cationic tetraoxides.[a]

	Neutral	Anion	Cation					
Cluster	M	M	M	EA_{ad}	VDE	Exp.[b]	IE	VIE
ScO_4	1	2	2	2.73	4.01		8.15	8.58
TiO_4	2	1	1	3.72	3.79		9.84	10.83
VO_4	1	0	2	3.43	4.04	4.0 ± 0.1	10.41	11.08
CrO_4	0	1	1	4.37	4.89	4.98 ± 0.09	10.14	10.66
MnO_4	1	0	2	4.89	5.00	4.96 ± 0.1	10.35	11.99
FeO_4	0	1	1	3.69	3.76	3.84 ± 0.04[c]	10.54	12.11
CoO_4	3	2	2	3.23	4.54		9.68	9.96
NiO_4	2	1	3	2.58	2.83		9.67	10.00
CuO_4	1	0	4	2.63	2.83	3.09 ± 0.04	8.77	9.28
ZnO_4	2	1	3	2.94	3.09		8.44	9.63

[a]All values are in eV except for the total magnetic moment values, which are in Bohr magnetons μ_B.
[b]See the experimental references in the text.
[c]The PES peak corresponding to the electron detachment from a FeO_4^- dioxo-peroxo isomer is located (Ref. 57) at 3.3 ± 0.04 eV.

EA_{ad} of TiO_4, CrO_4, MnO_4, and FeO_4 are 3.72 4.37, 4.89, and 3.69 eV, respectively, and are larger than the EA of Cl. The experimental values obtained from photoelectron detachment spectra of VO_4,[23] CrO_4,[19] MnO_4,[21] FeO_4,[57] and CuO_4[49] are given in Table II. As it is seen, the experimental values are close to our VDEs.

As mentioned above, the PES spectrum of FeO_4^- is likely to originate from two isomers with close total energies. Therefore, one could assume such a possibility for other tetraoxide anions. According to the results of our optimizations of the lowest total energy excited states, the differences E_{tot}(first excited state) – E_{tot}(ground state) in the tetraoxide anion series are 0.10 eV (Sc), 0.77 eV (Ti), 0.51 eV (V), 0.94 eV (Cr), 1.59 eV (Mn), 0.001 eV (Fe, three degenerate in total energy $^2A_1$, $^2B_1$, and $^2B_2$ states of D_{2d} symmetry), 0.08 eV (Co), 0.23 eV (Ni), 0.43 eV (Cu), and 0.49 eV (Zn). Therefore, one could likely expect the presence of isomers of Sc, Fe, Co, and Ni tetraoxide anions under certain experimental conditions. However, all the FeO_4^- isomers possess practically the same VDEs (3.74, 3.76, and 3.78 eV, respectively), and the PES peak at 3.3 ± 0.04 eV can be due to a dioxo-peroxo anion state $^4B_2$ (C_{2v}) which is above the triply generate doublet states by 0.72 eV. The presence of such an anion isomer, which is well separated from the ground state, could be related to the experimental conditions of the anion formation by attaching an extra electron to neutral species. The difference between a tetrahedral ground state of FeO_4 shown in Fig. 5 and a dioxo-peroxo $^2A_2$ (C_{2v}) state is only 0.04 eV, and both isomers may present in the neutral flow giving rise to two anion isomers. The E_{tot}(1th E.S.) – E_{tot}(G.S.) differences in the neutral tetraoxide series are 0.47 eV (Sc), 0.51 eV (Ti), 2.09 eV (V), 0.13 eV (V), 0.04 eV (Mn, $^2B_1$ and $^2A_1$ states of C_{2v} symmetry), 0.05 eV (Fe, a C_{2v} isomer), 0.21 eV, 0. 22 eV, and 0.30 eV (Co), 0.28 eV (Ni), 0.05 eV and 0.12 eV (Cu), and 0.09 eV (Zn). As it is seen, all late 3d-metal tetraoxides possess states that are close in total energy to the

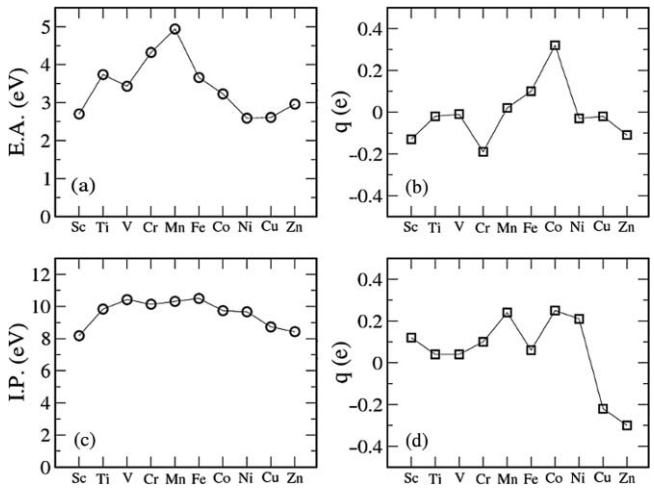

FIG. 6. The MO_4 series: (a) electron affinities; (b) differences in the metal atom charges of the MO_4 and MO_4^- pairs; (c) ionization energies; (d) differences in the metal atom charges of the MO_4^+ – MO_4 pairs.

corresponding ground states. The excited state data may be found in the supplementary material.[82]

According to the NBO analysis, the 3d-metal charge is positive in all MO_4 clusters. Figure 6(b) presents the metal charge variation in the anion series with respect to the metal atom charge in the ground-state MO_4 neutrals. As it is seen, there is no significant difference in the charge on the metal atoms. This implies that the extra electron is distributed over oxygen atoms in all MO_4^- anions. A noticeable exception presents CoO_4^- where the charge on the Co atom increases by ~0.3 e. The local magnetic moments at the metal sites of MO_4^- are small and do not exceed 0.6 μ_B (ScO_4^-).

C. MO_4^+ cations

The detachment of an electron from the neutral ground-state 3d-metal tetraoxides is accompanied by geometry changes in several cases. Thus, the peroxo groups of TiO_4 and VO_4 transform into the superoxo groups, while both peroxo groups of CuO_4 become the superoxo groups. Two oxo-atoms of MnO_4 and FeO_4 combine into the peroxo groups. Our ground state of VO_4^+ shown in Fig. 5 is similar to the state found previously[69] at B3LYP/6–3G* level. The electron detachment from a tetraoxide leads to either rupture of the bond between the metal and an oxygen atom or to a recombination of two oxo-atoms into a peroxo group.

The calculated IE and VIE values of all neutral MO_4 are given in Table II and plotted in Fig. 6(c). The values are rather close to each other when M = Sc, Cr, Co, or Ni, which is consistent with the small geometry changes due to the electron detachment (see Fig. 5). The differences between the metal atom charges in the neutral-cation pairs [q(neutral) – q(cation)] obtained from the NBO population analysis are presented in Fig. 6(d). As it is seen, there is no essential dependence of the metal atom charge on the 3d-metal tetraoxide charge. This implies that the detached electron originates from oxygen ligands. The largest differences are observed for the Cu and Zn pairs. This can be attributed to a decreasing interaction between the metal and oxygen atoms as it follows from the smaller fragmentation energies in Fig. 2(d). The total magnetic moments of the MO_4^+ cations are larger than the total magnetic moments of their neutral parents in a number of cases.

V. COMPARISON OF THE MO_3 AND MO_4 PROPERTIES

Our calculated fragmentation energies of the neutral and charged MO_3 and MO_4 species are compared in Fig. 7(a). As it is seen, the neutral trioxides are thermodynamically more stable than the neutral tetraoxides except for the Ni and Cu trioxides. That is, the metal oxide thermodynamic stability decreases when the oxygen content increases. The same conclusion is true for the negative ions as well since the anion fragmentation energies decrease when the oxygen content increases [see Fig. 7(b)].

The computed adiabatic electron affinities of the MO_3 and MO_4 clusters are compared in Fig. 7(d). The EA_{ad} of MnO_4 is substantially larger than the EA_{ad} of MnO_3 despite the MnO_4^- anion is thermodynamically less stable than the MnO_3^- anion. MnO_4 satisfies the formula for oxygen superhalogens and has the EA_{ad} that substantially exceeds the EA of the Cl atom. The EA_{ad}s of TiO_4, CrO_4, and FeO_4 are also larger than the EA of the Cl atom and they are superhalogens as well. To qualitatively analyze the superhalogen nature, we calculated the binding energy difference in the neutral–anion pairs plotted in Fig. 7(c). Comparing Figs. 7(c) and 7(d), one can find a strong correlation between the EA_{ad} value and the difference between the anion and neutral thermodynamic stability. The only exception presents the MnO_3–MnO_3^- pair. It is worth to mention that the largest difference in the binding energies found for the VO_3, MnO_3, CoO_3, CrO_4, MnO_4, and FeO_4 pairs correlates with the availability of the experimental photoelectron spectra for the corresponding anions.

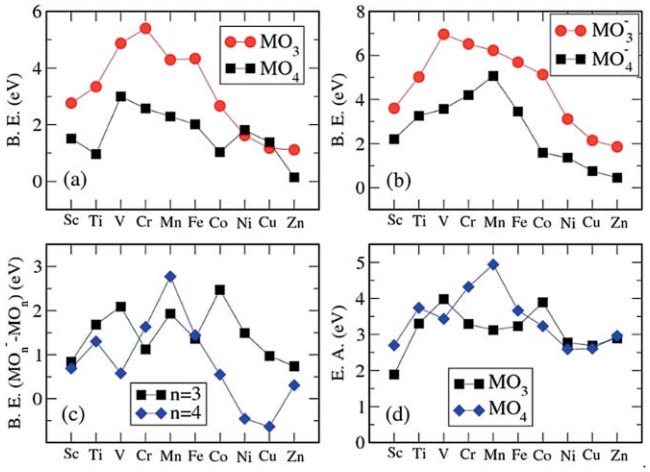

FIG. 7. Comparison of the binding energies (B.E.) for (a) MO_3 and MO_4 series and (b) MO_3^- and MO_4^- series; (c) differences in the binding energies of the MO_n^- and MO_n series, n = 3 and 4; (d) comparison of the adiabatic electron affinities in the neutral MO_3 and MO_4 series.

VI. CONCLUSION

We performed a systematic study of the neutral and singly negatively and positively charged trioxides and tetraoxides of 3d-metal atoms using density functional theory with generalized gradient approximation. The main results obtained can be summarized as follows:

(1) The ground-state geometries of neutral MO_3 change when moving from Sc to Zn trioxides. The preferred geometry in the beginning and the end of the series has an oxo-peroxo form, while all oxygen atoms are bound dissociatively in the middle of the series from V to Co. In the MO_4 series, the ground-state geometries have diperoxo (Sc, Co, Ni, Cu, and Zn), dioxo-peroxo (Ti, V, and Cr), and tetraoxo (Mn and Fe) topologies.
(2) The change in geometries due to the attachment or detachment of an electron is characteristic for the early and late 3d-metal atoms. An extra electron attachment transforms a peroxo group into two oxo-atoms or a superoxo group. On the contrary, an electron detachment can lead to a recombination of two oxo-atoms into a peroxo or superoxo group.
(3) The MO_4 binding energies defined as the smallest energies required for yielding atomic or molecular oxygen are smaller than the MO_3 binding energies. This can serve as an indicator that molecular oxygen will be less bound to the metal atom when the oxygen content increases.
(4) The adiabatic electron affinities of VO_3, CoO_3, TiO_4, CrO_4, MnO_4, and FeO_4 are larger than the electron affinity of the Cl atom and these species are superhalogens. VO_3 and MnO_4 satisfy the superhalogen formula and possess the largest electron affinities in the trioxide and tetraoxide series, respectively.
(5) The difference between binding energies in the MO_n – MO_n^- pairs is the largest for those pairs where the neutral oxide is a superhalogen.
(6) In the ZnO_n series (n = 1–4), only ZnO and ZnO_3 are thermodynamically stable, while both ZnO_2 and ZnO_4 form geometrically stable states, which are unstable with respect to release of molecular oxygen.
(7) The differences between our vertical electron detachment energies of an extra electron from the MO_3^- and MO_4^- anions obtained at the BPW91/6–311+G(3df) level and the corresponding experimental values obtained from the photoelectron spectra do not exceed 0.2 eV within the experimental uncertainty bars.

ACKNOWLEDGMENTS

This work was partially supported by a grant from the Defense Threat Reduction Agency (Grant No. HDTRA1–09-1–0025) and by a contract from the US Army Night Vision and Electronic Sensors Directorate. The research was also supported in part by the National Science Foundation through TeraGrid resources provided by NCSA. Portions of this research were conducted with high performance computational resources provided by the Louisiana Optical Network Initiative (http://www.loni.org).

[1] C. N. R. Rao and B. Raveau, *Transition Metal Oxides* (CVCH, New York, 1995).
[2] Y. Gong, M. F. Zhou, and L. Andrews, Chem. Rev. **109**, 6765 (2009).
[3] S. Riedel and M. Kaupp, Coord. Chem. Rev. **253**, 606 (2009).
[4] L. M. Ioffe, T. Lopez, Y. Borod'ko, and R. Gomez, J. Mol. Catal. A: Chem. **98**, 25 (1995).
[5] P. Jena and A. W. Castleman, Jr., Proc. Natl. Acad. Sci. U.S.A **103**, 10560 (2006).
[6] X. Lai and D. W. Goodman, J. Mol. Catal. A: Chem. **162**, 1647 (2000).
[7] D. F. Hunt, G. C. Stafford, Jr., F. W. Crow, and J. W. Russell, Anal. Chem. **48**, 2098 (1976).
[8] F. A. Cotton and G. Wilkinson, *Advanced Inorganic Chemistry* (Wiley-Interscience, New York, 1988).
[9] G. L. Gutsev, B. K. Rao, and P. Jena, J. Phys. Chem. A **104**, 5374 (2000).
[10] G. L. Gutsev, B. K. Rao, and P. Jena, J. Phys. Chem. A **104**, 11961 (2000).
[11] G. L. Gutsev and A. I. Boldyrev, Chem. Phys. Lett. **108**, 250 (1984).
[12] M. K. Scheller, R. N. Compton, and L. S. Cederbaum, Science **270**, 1160 (1995).
[13] G. L. Gutsev and A. I. Boldyrev, Chem. Phys. **56**, 277 (1981).
[14] G. L. Gutsev and A. I. Boldyrev, Adv. Chem. Phys. **61**, 169 (1985).
[15] X.-B Wang, C.-F. Ding, L.-S. Wang, A. I. Boldyrev, and J. Simons, J. Chem. Phys. **110**, 4763 (1999).
[16] I. Anusiewicz and P. Skurski, Chem. Phys. Lett. **358**, 426 (2002).
[17] K. Pradhan, G. L. Gutsev, and P. Jena, J. Chem. Phys. **133**, 144301 (2010).
[18] X. Yang, X.-B. Wang, L.-S. Wang, S. Q. Niu, and T. Ichiye, J. Chem. Phys. **119**, 8311 (2003).
[19] G. L. Gutsev, P. Jena, H.-J. Zhai, and L.-S. Wang, J. Chem. Phys. **115**, 7935 (2001).
[20] G. L. Gutsev, B. K. Rao, P. Jena, X. Li, and L.-S. Wang, J. Chem. Phys. **113**, 1473 (2000).
[21] G. L. Gutsev, B. K. Rao, P. Jena, X.-B Wang, and L.-S. Wang, Chem. Phys. Lett. **312**, 598 (1999).
[22] G. L. Gutsev, S. N. Khanna, B. K. Rao, and P. Jena, J. Phys. Chem. A **103**, 5812 (1999).
[23] H. B. Wu and L.-S. Wang, J. Chem. Phys. **108**, 5310 (1998).
[24] G. L. Gutsev, C. A. Weatherford, K. Pradhan, and P. Jena, J. Phys. Chem. A **114**, 9014 (2010).
[25] A. D. Becke, Phys. Rev. A **38**, 3098 (1988).
[26] J. P. Perdew and Y. Wang, Phys. Rev. B **45**, 13244 (1991).
[27] Y. Zhao and D. G. Truhlar, J. Phys. Chem. A **109**, 5656 (2005).
[28] S. F. Sousa, P. A. Fernandes, and M. J. Ramos, J. Phys. Chem. A **111**, 10439 (2007).
[29] K. E. Riley, B. T. Op't Holt, and K. M. Merz, Jr., J. Chem. Theory Comput. **3**, 407 (2007).
[30] G. L. Gutsev and C. W. Bauschlicher, Jr., J. Phys. Chem. A **107**, 7013 (2003).
[31] R. J. Bartlett and M. Musial, Rev. Mod. Phys. **79**, 291 (2007).
[32] S. Li and D. A. Dixon, J. Phys. Chem. A **112**, 6646 (2008).
[33] H.-J. Zhai, S. Li, D. A. Dixon, and L.-S. Wang, J. Am. Chem. Soc. **130**, 5167 (2008).
[34] S. Li, J. M. Hennigan, D. A. Dixon, and K. A. Peterson, J. Phys. Chem. A **113**, 7861 (2009).
[35] F. Grein, Int. J. Quantum Chem. **109**, 549 (2009).
[36] S. Li, H.-J. Zhai, L.-S. Wang, and D. A. Dixon, J. Phys. Chem. A **113**, 11273 (2009).
[37] R. Krishnan, J. S. Binkley, R. Seeger, and J. A. Pople, J. Chem. Phys. **72**, 650 (1980).
[38] A. D. Mclean and G. S. Chandler, J. Chem. Phys. **72**, 5639 (1980).
[39] M. J. Frisch, G. N. Trucks, H. B. Schlegel *et al.*, GAUSSIAN 03, *Revision B.04*, Gaussian, Inc., Pittsburgh, PA, 2003.
[40] A. E. Reed, L. A. Curtiss, and F. Weinhold, Chem. Rev. **88**, 899 (1988).
[41] C. W. Bauschlicher, Jr., M. F. Zhou, L. Andrews, J. R. T. Johnson, I. Panas, A. Snis, and B. O. Roos, J. Phys. Chem. A **103**, 5463 (1999).
[42] Y. Gong and M. F. Zhou, J. Phys. Chem. A **112**, 9758 (2008).
[43] E. Uzunova, J. Chem. Phys. A **115**, 1320 (2011).
[44] M. F. Zhou and L. Andrews, J. Chem. Phys. **111**, 4230 (1999).
[45] G. V. Chertihin, W. D. Bare, and L. Andrews, J. Chem. Phys. **107**, 2798 (1997).
[46] R. F. Ferrante, J. L. Wilkerson, W. R. M. Graham, and W. Weltner, Jr., J. Chem. Phys. **67**, 5904 (1977).
[47] Y. Gong and M. F. Zhou, J. Phys. Chem. A **112**, 10838 (2008).
[48] A. Citra, G. V. Chertihin, L. Andrews, and M. J. Neurock, J. Phys. Chem. A **101**, 3109 (1997).

[49]H. B. Wu, S. R. Desai, and L.-S. Wang, J. Phys. Chem. A **101**, 2103 (1997).
[50]G. V. Chertihin, L. Andrews, and C. W. Bauschlicher, Jr., J. Phys. Chem. A **101**, 4026 (1997).
[51]L. B. Knight, Jr., R. Babb, M. Ray, T. J. Banisaukas III, L. Russon, R. S. Dailey, and E. R. Davidson, J. Chem. Phys. **105**, 10237 (1996).
[52]E. Jakubikova, A. K. Rappe, and E. R. Bernstein, J. Phys. Chem. A **111**, 12938 (2007).
[53]A. Bande and A. Lüchow, Phys. Chem. Chem. Phys. **10**, 3371 (2008).
[54]E. L. Uzunova, G. St. Nikolov, and H. Mikosch, J. Phys. Chem. A **106**, 4104 (2002).
[55]G. L. Gutsev, L. Andrews, and C. W. Bauschlicher, Jr., Theor. Chem. Acc. **109**(6), 298 (2003).
[56]H. B. Wu and L.-S. Wang, J. Chem. Phys. **107**, 8221 (1997).
[57]H. B. Wu, S. R. Desai, and L.-S. Wang, J. Am. Chem. Soc. **118**, 7434 (1996).
[58]M. B. Walsh, R. A. King, and H. F. Schaefer III, J. Chem. Phys. **110**, 5224 (1999).
[59]V. T. Tran and M. F. A. Hendrickx, J. Chem. Theory Comput. **7**, 291(2011).
[60]K. Deng, J. Yang, and Q. Zhu, J. Chem. Phys. **113**, 7867 (2000).
[61]T. Baruah, R. R. Zope, and M. R. Pederson, Phys. Rev. A **69**, 023201 (2004).
[62]Y.-X. Zhao, X.-L. Ding, Y.-P. Ma, Z.-C. Wang, and S.-G. He, Theor. Chem. Acc. **127**, 449 (2010).
[63]J. F. Harrison, Chem. Rev. **100**, 679 (2000).
[64]Y. Nakao, K. Hirao, T. Taketsugu, J. Chem. Phys. **114**, 7935 (2001).
[65]E. Miliordos and A. J. Mavridis, J. Phys. Chem. A **111**, 1953 (2007).
[66]M. Pykavy and C. Van Wullen, J. Phys. Chem. A **107**, 5566 (2003).
[67]M. Brümmer, C. Kaposta, G. Santambrogio, and K. R. Asmis, J. Chem. Phys. **119**, 12700 (2003).
[68]K. R. Asmis, G. Meijer, M. Brümmer, C. Kaposta, G. Santambrogio, L. Wöste, and J. Sauer, J. Chem. Phys. **120**, 6461 (2004).
[69]M. Calatayud, B. Silvi, J. Andrés, and A. Beltrán, Chem. Phys. Lett. **333**, 493 (2001).
[70]G. K. Koyanagi, D. K. Bohme, I. Kretzschmar, D. Schröder, and H. Schwarz, J. Phys. Chem. A **105**, 4259 (2001).
[71]S. Riedel and M. Kaupp, Coord. Chem. Rev. **253**, 606 (2009).
[72]Y. Gong and M. F. Zhou, Phys. Chem. Chem. Phys. **11**, 8714 (2009).
[73]Y. Gong, C. F. Ding, and M. F. Zhou, J. Phys. Chem. A **111**, 11572 (2007).
[74]M. F. Zhou and L. Andrews, J. Phys. Chem. A **102**, 8251 (1998).
[75]Y. Zhao, Y. Gong, M. H. Chen, and M. F. Zhou, J. Phys. Chem. A **110**, 1845 (2006).
[76]Y. Gong, G. J. Wang, and M. F. Zhou, J. Phys. Chem. A **112**, 4936 (2008).
[77]Y. Gong, M. F. Zhou, and L. Andrews, J. Phys. Chem. A **111**, 12001 (2007).
[78]G. L. Gutsev, S. N. Khanna, B. K. Rao, and P. Jena, Phys. Rev. A **59**, 3681 (1999).
[79]D. Danset, M. E. Alikhani, and L. Manceron, J. Phys. Chem. A **109**, 105 (2005).
[80]C. Massobrio and Y. Pouillon, J. Chem. Phys. **119**, 8305 (2003).
[81]H. Wu and L.-S. Wang, J. Phys. Chem. A **102**, 9129 (1998).
[82]See supplementary material at http://dx.doi.org/10.1063/1.3570578 for the concise data on all ground and lowest total energy excited states optimized in the present work.